

1S_0 pairing correlations in relativistic nuclear matter and the two-nucleon virtual state

B. V. Carlson and T. Frederico

Departamento de Física, Instituto Tecnológico da Aeronáutica – CTA, 12.228-900 São José dos Campos, São Paulo, Brazil

F.B. Guimarães

EAN – Instituto de Estudos Avançados – CTA, 12.228-840 São José dos Campos, São Paulo, Brazil

We use the Gorkov formulation of the Dirac-Hartree-Fock-Bogoliubov approximation to nuclear pairing to study the 1S_0 nucleon-nucleon correlations in nuclear matter. We find the short-range correlations of the 1S_0 pairing fields to be almost identical to those of the two-nucleon virtual state. We obtain mutually consistent results for the pairing fields, using several different sets of effective interaction parameters, when we demand that each of these sets places the virtual-state pole at its physical location.

The non-relativistic BCS and Hartree-Fock-Bogoliubov (HFB) approximations have been used with success to study pairing in nuclear physics, both years ago [1–7] and still today [8–16]. Pairing approximations provide a simple means of extending the independent-particle approximation to one which includes the effects of the binding energy and short-range correlations associated with bound pairs of nucleons in the nuclear medium. The long-range correlations associated with collective phenomena in nuclei are similarly described using the non-relativistic random-phase approximation (RPA).

On the other hand, it is well known that non-relativistic independent-particle approaches using realistic two-body interactions have difficulties in accounting for basic phenomena, such as the spin-orbit part of the nucleon-nucleus interaction and the saturation properties of nuclear matter. These properties can be fairly easily described in a relativistic formulation, in which effective mesons are exchanged between Dirac nucleons. The success of the relativistic mean field approach, initially developed by Walecka and collaborators and later by many others [17–24], invited its extension to approximations that could take into account the residual correlations between nucleons.

Consistent relativistic formulations of both the RPA and the HFB [25–28] have thus been developed. Of the latter, the authors of Ref. [25] derived self-consistent equations for the components of the relativistic pairing field but performed no calculations. The results obtained in Refs. [26] and [27], using a zero-range model and a non-relativistic reduction of the pairing equations, respectively, are generally much larger than those obtained in non-relativistic calculations, although both of the relativistic calculations used interaction parameters that were fit to yield the saturation point of nuclear matter. Such results would indicate that other aspects of the interaction are involved in pairing than those necessary to describe the bulk characteristics of nuclei and of nuclear matter. The crudeness of the calculations, however, do not permit a firm conclusion to be reached. The results obtained in the fully relativistic finite-range calculations of Ref. [28] are very similar and do permit such a conclusion. Here we will show that, in addition to describing the bulk properties of nuclear matter, a nucleon-nucleon interaction must provide a good description of the two-nucleon 1S_0 virtual state, if it is to furnish a good description of 1S_0 pairing in nuclear matter.

The HFB approximation introduces short-range two-nucleon correlations through the pairing fields and their momentum dependence. These correlations have been investigated in recent years in non-relativistic models of nuclear pairing. [11,14–16] In particular, the close association between the short-range correlations of the two-nucleon 1S_0 virtual state and those of the 1S_0 pairing fields was investigated in Ref. [15]. We investigate the same association in the relativistic model and reach a similar but stronger conclusion: the short-range correlations of the pairing field are almost identical to those of the two-nucleon virtual state. For the relativistic interactions we have used, the short-range repulsion and medium-range attraction resulting from the exchange of effective mesons provide a description of the short-range correlations in very good agreement with those of the two-nucleon virtual state, deduced from realistic nucleon-nucleon potential models. By requiring that the interactions also reproduce the position of the virtual state pole or, equivalently, the two-nucleon singlet scattering length, we will show that the effective relativistic interactions can provide a consistent description of pairing, both among themselves and with the non-relativistic calculations.

PAIRING AND TWO-NUCLEON CORRELATIONS

In a two-particle system, bound-state correlations can be roughly classified as asymptotic ones and short-range ones. The asymptotic ones are determined principally by the binding energy, while the short-range ones depend on

the high-momentum components of the wave function. This can be seen by examining the manner in which a bound pair appears in the two-body T-matrix, $T(E)$. The T-matrix satisfies the integral equation

$$T(E) = V + V G_0(E) T(E), \quad (1)$$

where V is the two-body interaction and $G_0(E)$ the free two-body propagator. A bound state appears in the T-matrix as a pole at a negative value of the energy, $E = -\epsilon_b$, where ϵ_b is the binding energy of the pair. We then have

$$T(E) = d \frac{1}{E + \epsilon_b} d^\dagger + T_c(E), \quad (2)$$

with $T_c(E)$ the continuum (positive energy) part of the T-matrix and d the bound-state vertex function. Substitution of the latter expression into the integral equation immediately yields an equation for the vertex function,

$$d = V G_0(-\epsilon_b) d. \quad (3)$$

The vertex function describes the momentum dependence (spatial dependence) of the bound state and is closely related to its wavefunction. By rewriting the equation for the vertex function as

$$d = (-\epsilon_b - H_0) G_0(-\epsilon_b) d = V G_0(-\epsilon_b) d, \quad (4)$$

we can identify the bound-state wave function as $\psi = G_0(-\epsilon_b) d$. In this last expression, we can see the rough division of the correlations into asymptotic ones determined by the singularity of the Green's function, $G_0(-\epsilon_b)$, and short-range ones contained in the high momentum components of the vertex function, d .

The two-nucleon system in the vacuum has a bound state in the isospin one, 3S_1 - 3D_1 channel — the deuteron. In the isospin zero, 1S_0 channel, where we will study pairing, the two-nucleon system in the vacuum has no bound state. It does have a virtual state, however, with $k_v \approx -0.05i \text{ fm}^{-1}$ and $\epsilon_v = k_v^2/M \approx 140 \text{ keV}$, corresponding to a two-nucleon singlet scattering length $a_0 = 1/|k_v| \approx 23 \text{ fm}$. An expansion similar to that of Eq. (2) can still be performed to extract the contribution to the T-matrix of the virtual state. Because the energy of this state is extremely small, its contribution to the T-matrix dominates the low-energy scattering and essentially determines the short-range correlations in the 1S_0 channel. The short-range correlations determined by the momentum dependence of the vertex function of the virtual state, $d_v(q)$, are thus to good approximation given by the momentum dependence of the half-on-shell 1S_0 T-matrix at zero energy, $t_{10}(q, 0; 0)$. We have from the expression analogous to Eq. (2),

$$t_{10}(q, 0; 0) = \langle q | T_{10}(E = 0) | k = 0 \rangle \approx \langle q | d_v \rangle \frac{1}{\epsilon_v} \langle d_v | 0 \rangle. \quad (5)$$

Note that the asymptotic properties of the virtual state also play a role here, by determining the magnitude of the contribution of the virtual state to the T-matrix through the factor $1/\epsilon_v$. The short-range correlations contained in the q -dependence can be extracted unambiguously, however, by normalizing both sides of the equation to their values at $q = 0$.

To look for general two-particle correlations in nuclear matter, one could study the Brueckner \mathcal{G} -matrix. In this generalization of the two-particle T-matrix of Eq. (1), the propagator $G_0(E)$ is now a many-body operator that, beside describing the two-body propagation, must take into account the effects of Pauli blocking and of interaction with the nuclear medium. To look for bound-state correlations, one would examine the poles and respective vertex functions of the \mathcal{G} -matrix as advocated years ago by Emery [2,3]. Such an approach has been used by various authors [29–31]. We will use instead the HFB approximation. It too has been used to study bound-state correlations in nuclear matter [11,15,16] and to even estimate deuteron production in heavy-ion collisions [14].

We can lend force to our use of the HFB approximation to study bound-state correlations by analyzing qualitatively the manner in which the one-body HFB approach takes into account the two-body pairing bound state. We begin by observing that a bound-state vertex function d of the T- or \mathcal{G} -matrix can be considered as an operator that converts a two-body bound state into two single particles. We could instead consider this a one-body operator by (1) neglecting the particle number of the bound state and (2) considering one of the outgoing particles as an entering hole. The effect of the vertex function would then be the conversion of a hole to a particle. This is just what the pairing field, Δ , of the HFB approximation does. Analogously, we can associate the adjoint vertex function, d^\dagger , which converts two single particles to the two-body bound state, with the conjugate pairing field, $\bar{\Delta}$, which converts a particle to a hole.

To obtain a complete one-body description, we must take into account the propagation of particles and holes as well as the conversion of one to the other. A HFB formalism that succeeds in unifying these ingredients simply and clearly is the Gorkov one [32]. Although infrequently used in non-relativistic studies of pairing, the formalism has

served as the basis for various relativistic studies [25,27,28]. This is due, at least in part, to its natural expression in terms of the propagator language common to field-theoretical approaches.

The Gorkov formulation of pairing extends the usual particle propagator $G(x-x')$ to one of the form

$$\begin{pmatrix} G(x-x') & F(x-x') \\ \tilde{F}(x-x') & \tilde{G}(x-x') \end{pmatrix},$$

in which $\tilde{G}(x-x')$ describes the propagation of holes in the medium and the anomalous propagator $F(x-x')$ and its conjugate $\tilde{F}(x-x')$ describe the conversion of holes to particles and particles to holes, respectively. Inverting the reasoning that lead us from the vertex function d to the pairing field Δ , we can interpret the anomalous propagator and its conjugate as terms describing the overlap between the two-particle bound state and the two single particles. We thus expect the anomalous propagators to contain information about the relative motion of the two particles in the bound pair.

THE GORKOV FORMALISM

We sketch here the development of a Dirac version of Gorkov's self-consistent particle-hole propagator [28]. To do this, we begin with the following ansatz to the effective single-particle Lagrangian,

$$\begin{aligned} \int dt L_{eff} = \int d^4x d^4x' \{ & \bar{\psi}(x)(i\gamma_\nu \partial^\nu - M)\psi(x)\delta(x-x') + \mu\bar{\psi}(x)\gamma_0\psi(x)\delta(x-x') \\ & - \bar{\psi}(x)\Sigma(x-x')\psi(x') + \frac{1}{2}\bar{\psi}(x)\Delta(x-x')\psi_T(x') + \frac{1}{2}\bar{\psi}_T(x)\bar{\Delta}(x-x')\psi(x') \}, \end{aligned} \quad (6)$$

where Σ is the usual self-energy, Δ and $\bar{\Delta}$ are the pairing fields and μ is a chemical potential, which will be used to constrain the average baryon density.

The hole wave function, ψ_T , is defined as

$$\psi_T = B\bar{\psi}^T \qquad \bar{\psi}_T = \psi^T B^\dagger, \quad (7)$$

where ψ^T denotes the transpose of the wave function ψ , and the matrix $B = \tau_2 \otimes \gamma_5 C$, in which the Pauli matrix τ_2 acts in the isospin space and C is the charge conjugation matrix. We note that, up to a factor of γ_0 and a phase, the isospin doublet ψ_T is the time-reverse of ψ .

The requirement that the effective Lagrangian be Hermitian yields the following conditions on the self-energy and pairing fields,

$$\Sigma(x) = \gamma_0 \Sigma^\dagger(-x) \gamma_0 \qquad \text{and} \qquad \Delta(x) = \gamma_0 \bar{\Delta}^\dagger(-x) \gamma_0. \quad (8)$$

The requirement of invariance under transposition of the pairing terms yields the additional conditions

$$\Delta(x) = -B^T \Delta^T(-x) B^\dagger \qquad \text{and} \qquad \bar{\Delta}(x) = -B \bar{\Delta}^T(-x) B^*. \quad (9)$$

These constraints are important in limiting the possible structure of the self-energy and pairing fields.

Making use of the relation between ψ_T and $\bar{\psi}$, we can manipulate the effective one-particle Lagrangian into a matrix form,

$$\begin{aligned} \int dt L_{eff} = \frac{1}{2} \int d^4x d^4x' \quad & (\bar{\psi}(x), \bar{\psi}_T(x)) \times \\ & \begin{pmatrix} (i\gamma_\nu \partial^\nu - M + \mu\gamma_0)\delta(x-x') - \Sigma(x-x') & \Delta(x-x') \\ \bar{\Delta}(x-x') & (i\gamma_\nu \partial^\nu + M - \mu\gamma_0)\delta(x-x') + \Sigma_T(x-x') \end{pmatrix} \begin{pmatrix} \psi(x') \\ \psi_T(x') \end{pmatrix}, \end{aligned} \quad (10)$$

where

$$\Sigma_T(x) = B \Sigma^T(-x) B^\dagger. \quad (11)$$

The extended vector wave function is that of the quasi-particle. Its equation of motion is evident and could be written down immediately.

Due to the translational invariance of nuclear matter, the equation in momentum-space is diagonal in the wave number. For the momentum-space representation of the corresponding generalized Feynman propagator, the equation of motion takes the form

$$\begin{pmatrix} \gamma_\nu k^\nu - M - \Sigma(k) + \mu\gamma_0 & \Delta(k) \\ \bar{\Delta}(k) & \gamma_\nu k^\nu + M + \Sigma_T(k) - \mu\gamma_0 \end{pmatrix} S_F(k) = 1. \quad (12)$$

We note that the momentum-dependent unitary transformation that diagonalizes the matrix operator is the Dirac version of the Bogoliubov-Valantin transformation.

To make contact between the effective quasi-particle Lagrangian and an interacting one, we assume that the meson+interaction terms in the latter have been reduced to four-fermion terms of the following form,

$$\int dt L_I = \frac{1}{2} \int d^4x d^4x' \bar{\psi}(x) \Gamma_\alpha(x) \psi(x) D^{\alpha\beta}(x-x') \bar{\psi}(x') \Gamma_\beta(x') \psi(x'), \quad (13)$$

where $\Gamma_\alpha(x)$ and $\Gamma_\beta(x')$ are vertex functions, $D^{\alpha\beta}(x-x')$ is the meson propagator, and α and β represent any indices necessary for the correct description of the meson propagation and coupling.

We can obtain the mean field contribution of this interaction term by replacing each of the possible pairs of fermion fields by its ground-state expectation value,

$$\begin{aligned} \int dt (L_I)_{eff} = \frac{1}{2} \int d^4x d^4x' D^{\alpha\beta}(x-x') \{ & 2\bar{\psi}(x) \Gamma_\alpha(x) \psi(x) \langle \bar{\psi}(x') \Gamma_\beta(x') \psi(x') \rangle > \\ & + 2\bar{\psi}(x) \Gamma_\alpha(x) \langle \psi(x) \bar{\psi}(x') \rangle > \Gamma_\beta(x') \psi(x') \\ & - \bar{\psi}(x) \Gamma_\alpha(x) \langle \psi(x) \psi^T(x') \rangle > \Gamma_\beta^T(x') \bar{\psi}^T(x') \\ & - \psi^T(x) \Gamma_\alpha^T(x) \langle \bar{\psi}^T(x) \bar{\psi}(x') \rangle > \Gamma_\beta(x') \psi(x') \}, \end{aligned} \quad (14)$$

where, by $\langle \dots \rangle$, we mean the time-ordered ground-state expectation value, $\langle 0 | T(\dots) | 0 \rangle$.

We note that the first term in this expression is a Hartree one and the second a Fock exchange one, while the last two, after using the definition of ψ_T to replace the transposed ψ 's, can be recognized as pairing terms. Comparing these mean field contributions to those of the effective quasi-particle Lagrangian, we can express the self-energy and pairing fields in terms of the two-fermion ground-state expectation values as

$$\begin{aligned} \Sigma(x-x') = -\delta(x-x') \Gamma_\alpha(x) \int d^4x'' D^{\alpha\beta}(x-x'') \langle \bar{\psi}(x'') \Gamma_\beta(x'') \psi(x'') \rangle & \\ -\Gamma_\alpha(x) D^{\alpha\beta}(x-x') \langle \psi(x) \bar{\psi}(x') \rangle > \Gamma_\beta(x') & \end{aligned} \quad (15)$$

and

$$\Delta(x-x') = -\Gamma_\alpha(x) D^{\alpha\beta}(x-x') \langle \psi(x) \bar{\psi}_T(x') \rangle > B \Gamma_\beta^T(x') B^\dagger, \quad (16)$$

where the equation for $\bar{\Delta}$ can be obtained using the Hermiticity condition of Eq. (8). These expressions become self-consistency equations when we evaluate the expectation values by using their relationship to the quasi-particle propagator,

$$iS_F(x-x') = i \begin{pmatrix} G(x-x') & F(x-x') \\ \tilde{F}(x-x') & \tilde{G}(x-x') \end{pmatrix} = \left\langle \begin{pmatrix} \psi(x) \\ \psi_T(x) \end{pmatrix} (\bar{\psi}(x'), \bar{\psi}_T(x')) \right\rangle, \quad (17)$$

which is itself a function of the mean fields.

The equations in momentum space are obtained by Fourier transforming the above expressions, giving

$$\begin{aligned} \Sigma(k) = \Gamma_\alpha(0) D^{\alpha\beta}(0) \int \frac{d^4q}{(2\pi)^4} \text{Tr} [\Gamma_\beta(0) G(q)] e^{iq^0 0^+} & \\ - \int \frac{d^4q}{(2\pi)^4} \Gamma_\alpha(q) D^{\alpha\beta}(q) G(k-q) \Gamma_\beta(-q), & \end{aligned} \quad (18)$$

and

$$\Delta(k) = - \int \frac{d^4q}{(2\pi)^4} \Gamma_\alpha(q) D^{\alpha\beta}(q) F(k-q) B \Gamma_\beta^T(-q) B^\dagger. \quad (19)$$

To complete the set of equations, we include that constraining the baryon density,

$$\rho_B = \langle \bar{\psi} \gamma_0 \psi \rangle = \int \frac{d^4q}{(2\pi)^4} \text{Tr} [\gamma_0 G(q)] e^{iq^0 0^+}. \quad (20)$$

Solving the self-consistency equations in conjunction with this constraint, we obtain the nonperturbative self-energy and pairing fields.

Here, we restrict our attention to 1S_0 pairing in symmetric nuclear matter. The Hermiticity and transposition invariance conditions of Eqs. (8) and (9), as well as the requirements of invariance under Lorentz and parity transformations reduce the possible form of the self-energy field to

$$\Sigma(k) = \Sigma_S(k) - \gamma_0 \Sigma_0(k) + \vec{\gamma} \cdot \vec{k} \Sigma_V(k), \quad (21)$$

while we take the form of the pairing field to be

$$\Delta(k) = \bar{\Delta}(k) = (\Delta_S(k) - \gamma_0 \Delta_0(k) - i\gamma_0 \vec{\gamma} \cdot \vec{k} \Delta_T(k)) \vec{\tau} \cdot \hat{n}. \quad (22)$$

Both the self-energy and pairing terms have Lorentz scalar and time-like vector components. To be consistent with our assumption of symmetric nuclear matter, the self-energy must be an isoscalar. The transposition invariance condition of Eq. (9) forces the scalar pairing field to be an isovector. We have simplified the form of the pairing field by assuming that it can be taken to be real and that the isospin dependence can be isolated in an overall factor of $\vec{\tau} \cdot \hat{n}$, where the unit vector \hat{n} is arbitrary. The special case $\vec{\tau} \cdot \hat{n} = \tau_2$ corresponds to the standard one of proton-proton and neutron-neutron pairing. Although we have not studied more elaborate isospin dependences, we have examined complex solutions to the pairing equations and found them to differ by only an overall phase from the solutions restrained to be real.

After substituting the simplified expressions for the mean fields into the propagator and the self-consistency equations, the latter can be reduced to coupled equations for the components of the mean fields and the chemical potential, μ . The self-consistency equations contain contributions from both the negative-energy and the positive-energy states (from the Dirac sea and the Fermi sea). To avoid the complications of renormalization, we have discarded the poles of the HFB propagator corresponding to negative-energy states. This procedure is not equivalent to the neglect of the HF negative-energy states performed in Ref. [27], nor are the differences small, as one might first expect. The contribution to the HFB states of the negative-energy HF states reduces the magnitude of the pairing fields, much as the contribution to the HF states of the negative-energy free states reduces the attractive scalar component of the HF mean field. More details can be found in Ref. [28], where we compare the two approximations and show that discarding the HFB negative-energy states yields much more reasonable results.

NUMERICAL RESULTS AND DISCUSSION

We have performed calculations of 1S_0 pairing in symmetric nuclear matter for various sets of interaction parameters (meson-nucleon coupling constants and meson masses [17–19]). We introduced, as an additional parameter, a momentum cutoff at $|\vec{k}| = \Lambda$ (in the nuclear matter rest frame), which limits the momentum integrations in the self-consistency equations. Such a cutoff could be considered a crude approximation to the nucleon-meson vertex form factors that our calculations do *not* contain. We performed calculations for various values of the momentum cutoff.

As the self-consistency equations for the pairing fields are proportional to the pairing fields, it is always possible to find a solution in which these fields are null. This zero pairing-field solution is just the normal HF one. In our calculations, we have found this to be the only self-consistent solution at sufficiently high baryon density. At densities lower than about two thirds of the saturation density, $\rho_B \leq 2\rho_{B0}/3$, we also find a non-trivial HFB solution. (We will not consider the region of exponentially small pairing fields discussed in Ref. [15].)

We display, in Fig. 1, the two principal components of the pairing field, $\Delta_S(k_F)$ and $\Delta_0(k_F)$, evaluated at the Fermi momentum, obtained for two different values of the momentum cutoff Λ using the σ - ω model parameters of Ref. [19]. The third component of the pairing field, Δ_T , is three orders of magnitude smaller than Δ_S and Δ_0 and is not shown. The components of the pairing field are plotted as functions of the Fermi momentum, where the latter is *defined* through its standard relation to the baryon density, that is, $\rho_B = \gamma k_F^3 / 6\pi^2$ where γ is 2 for nuclear matter and 1 for neutron matter. We observe that the magnitudes of the components of the pairing field, represented here

by their values at the Fermi momentum, $\Delta_{0,s}(k_F)$, depend strongly on the Fermi momentum (and thus the baryon density). In both of the cases shown, which are typical ones, the fields increase rapidly at small densities, reach a maximum at about 1/4 the saturation density, and fall back to zero before the saturation density is reached. We observe that the magnitude of the components of the pairing field also clearly depend on the value of the momentum cutoff. The form of the functional dependence of the fields on the Fermi momentum, however, is fairly insensitive to the value of the cutoff.

Diagonalizing the equation of motion, Eq. (12), in the particle-particle and hole-hole subspaces — equivalent to expanding in the HF basis in these subspaces — reduces the pairing fields to effective ones for the positive- and negative-energy states and to a coupling term which is small for low momenta (but increases with the momentum) [28]. The effective pairing field for the positive-energy states, which we call the gap function, is

$$\Delta_g(k) = \frac{M^*(k)}{E_k^*} \Delta_0(k) - \Delta_S(k) + i \frac{k^* |\vec{k}|}{E_k^*} \Delta_T(k), \quad (23)$$

where $k^* = (1 + \Sigma_V(k))|\vec{k}|$, $M^* = M + \Sigma_0(k)$, and $E^* = \sqrt{k^{*2} + M^{*2}}$. This is the quantity whose role is closest to that of the non-relativistic pairing field. Like the non-relativistic self-energy, it too is the difference between two larger relativistic quantities. This is evident in Fig. 1, in which the gap functions for the two different values of the momentum cutoff are displayed together with the components of the pairing field. We observe that different values of the momentum cut-off result in gap functions Δ_g of different magnitude but with approximately the same form of functional dependence on the Fermi momentum. The gap functions are quite similar, in form, to those obtained in various non-relativistic calculations using realistic potentials [9,15,16,30].

In Fig. 2, we compare the components of the pairing field and gap functions obtained using the parameters of Ref. [18] and Ref. [19], at a fixed value of the cutoff momentum Λ , again in a σ - ω model. Here, we observe that different values of the interaction parameters also result in pairing fields Δ_0 and Δ_s and gap functions Δ_g of different magnitudes but, again, with roughly the same form of functional dependence on the Fermi momentum.

As we expect the pairing fields and the gap function, like the two-nucleon vertex function, to contain only short-range two-nucleon correlations, we expect their dependence on the momentum to be approximately the same over a wide range of nuclear densities. We would expect significant changes in their momentum dependence only at densities high enough for the probability to become appreciable of a third nucleon to be found simultaneously with the pair within the effective radius of about 0.5 fm that is characteristic of the short-range correlations. In Fig. 3, we show the normalized momentum dependence of the pairing fields and gap function (at a fixed value of the Fermi momentum), $\Delta(k)/\Delta(0)$, obtained using the interaction parameters of Ref. [19] and a momentum cutoff of $\Lambda = 2$ GeV/c, for several values of the baryon density. The curve corresponding to zero density gives the momentum dependence of the virtual state solution to the vacuum pairing equations, which is discussed below. Confirming our expectations, at low density, we find that the momentum dependence of the pairing fields and gap function is indeed almost independent of the density. As the density increases, differences begin to appear in the gap function but remain small almost up to the density at which pairing disappears. The momentum dependence of the pairing fields remains almost identical to that of the virtual state over the entire range of densities for which pairing occurs.

We note that in Ref. [15] a similar comparison was made of the momentum dependence of the non-relativistic gap function at various values of the baryon density, but for the case of neutron matter. They observed slightly larger variations of the normalized gap function than the ones we have found but, as their calculations were non-relativistic, did not observe the invariance of the pairing fields. Our results for neutron matter are almost identical to those in Fig. 3 and are not shown here. We want to emphasize, however, that the momentum dependence of the neutron matter pairing fields is just as independent of the matter density as is the momentum dependence of the pairing fields in the case of nuclear matter.

We would also like the short-range correlations contained in the pairing fields and gap function to be relatively independent of the interaction parameters, at least if we believe that these parameters provide a reasonable description of the actual physical situation. We can see in Fig. 4 that, to a certain extent, this is the case. There we show the normalized momentum dependence of the pairing fields and gap function, obtained for two different values of the momentum cutoff using the σ - ω model parameters of Ref. [18] and of Ref. [19]. We see that the normalized momentum-dependence of the pairing fields and gap function, although similar, is clearly different for the two sets of interaction parameters. However, the momentum-dependence of the fields depends only weakly on the values of the cutoff, Λ , as is also the case for the other sets of interaction parameters that we have used.

In the limit of zero density, the integral equation for the pairing field, Eq. (19), reduces to the ladder approximation to the Bethe-Salpeter equation for a two-particle bound state, in which the the chemical potential is identified with the two-body bound-state energy and antiparticle propagation in the two-nucleon center-of-mass frame has been discarded. For a physically reasonable interaction, this has no nontrivial solution in the 1S_0 channel, as the two-nucleon system has no bound state there. The 1S_0 virtual state appears as a solution when the equation is analytically extended to

the second energy sheet. As we have already stated, the energy of the virtual 1S_0 -state is extremely small, so that its vertex function dominates the short-range correlations in two-nucleon scattering at low energies. As the virtual state and the pair state at low nuclear matter densities are solutions of essentially the same equation (and contain essentially the same physics), we expect the short-range correlations of the pair state to be similarly dominated by the short-range correlations of the virtual state. We thus expect the the components of the pairing field to have a momentum dependence similar to that of the components of the vertex function of the virtual state. We have seen in Fig. 3 that, at low densities, this is indeed the case. As the gap function Δ_g has a momentum dependence similar to that of the non-relativistic vertex function of the virtual state $d_v(q)$ we expect, as discussed above, that it should also have a dependence on the momentum similar to that of the half-on-shell matrix element of the zero-energy non-relativistic 1S_0 T-matrix, $t_{10}(q, 0; 0)$. That is, we expect that

$$\frac{\Delta_g(q)}{\Delta_g(0)} \approx \frac{d_v(q)}{d_v(0)} \approx \frac{t_{10}(q, 0; 0)}{t_{10}(0, 0; 0)}. \quad (24)$$

In Figs. 3 and 4, we have plotted, together with the normalized pairing fields, the normalized non-relativistic zero-energy half-on-shell 1S_0 T-matrix, for the case of the Bonn-B potential [33], which includes the exchange of σ , ω , ρ , π , η and δ mesons between nucleons. We see in Fig. 3, for the interaction parameters of Ref. [19], that the agreement between the ratios of gap functions and half-on-shell T matrices is quite good. We observe in Fig. 4 that the ratios of gap functions for the interaction parameters of Ref. [18] do not agree quite as well as those of Ref. [19] with the ratios of half-on-shell T matrices, although they are still quite similar, as are the gap functions of the other sets of interaction parameters. We thus conclude that the momentum dependence of the effective interactions that we used does provide a reasonable description of the actual physical situation.

In contrast with the almost unchanging momentum dependence of the pairing fields, we find that their magnitudes depends strongly on the interaction parameters and the value of the cutoff. This reflects the fact that nuclear pairing is the result of a delicate balance between short-range repulsion and long-range attraction. [13] Changing the interaction parameters or the momentum cutoff changes the point of this balance, modifying the magnitudes of the fields. However, such modifications do not appear in the magnitudes of the pairing fields alone. As we have noted, in the zero density limit, the equation for the pairing field, Eq. (19), reduces to the ladder approximation to the Bethe-Salpeter equation for a two-particle bound state in the 1S_0 channel. For some sets of interaction parameters and momentum cutoff, a bound state can indeed be found. In other cases, where no bound state exists, analytic continuation of the pairing equations to the second energy sheet reveals a virtual state in the 1S_0 channel.

We find the magnitudes of the gap function and the pairing fields at low densities to be strongly correlated with the location in the complex momentum plane of the virtual state or bound state in the vacuum that is produced by each set of interaction parameters + cutoff. We display these correlations in Figs. 5 and 6, where comparison is made between several different parameter sets with varying numbers of mesons. Calculations were performed including the σ , ω , ρ and π mesons and also including just the σ - ω mesons, as the latter dominate the gross features of the pairing fields and gap function. Calculations were also performed using a relativistic zero-range interaction, in which the σ and ω mesons are taken to be infinitely heavy and the coupling constants are defined so as to yield the correct nuclear-matter saturation point. For each parameter set, the momentum cutoff Λ was varied with all other parameters kept fixed. For each value of the momentum cutoff, we determined the pairing gap at $k_F=0.5 \text{ fm}^{-1}$, about 1/8 of the saturation density, and obtained the bound or virtual state energy in the vacuum.

We observe in Figs. 5 and 6 that the value of the free two-nucleon bound or virtual state energy essentially determines the magnitudes of the gap function $\Delta_g(k_F)$ and the pairing fields $\Delta_{0,s}(k_F)$ at $k_F=0.5 \text{ fm}^{-1}$. The σ - ω results agree well among themselves, with their values for each of the pairing fields and gap function all lying within a narrow band. Although the inclusion of other mesons increases the size of the bands, their widths still remain small relative to the magnitudes of the fields. In Fig. 5, we see that even the zero-range model yields results for the gap function in good agreement with those of the other calculations. However, it cannot reproduce the values of the components of the pairing field, $\Delta_{0,s}(k_F)$, obtained with the finite-range models, as is apparent in Fig. 6.

The correlations between the components of the pairing field, $\Delta_{0,s}(k_F)$, and the position of the virtual state, shown in Fig. 6, yield two distinct lines. In each case, one of these lines contains most of the finite-range results while the other contains the zero-range calculations. Several of the finite-range points lie between the two lines. The finite-range calculations that fall close to the zero-range line all correspond to extremely low values of the momentum cutoff, $\Lambda \lesssim 500 \text{ MeV}/c$. They are thus similar to the momentum-independent zero-range results in the sense that the pairing fields (but not the gap function) in these cases vary little as a function of the momentum. (Better said, they have very little room in which to vary.) This is clear from the leftmost portions of Figs. 3 and 4, in which the momentum dependence expected of the pairing fields for values of the cutoff $\Lambda \lesssim 500 \text{ MeV}/c$ is displayed in the range of values $k \lesssim 2.5 \text{ fm}^{-1}$.

We can understand better the correlation between the magnitudes of the pairing fields and the location of the

virtual state if we examine the coherence length of the pairing fields. The coherence length ξ of a bound pair is defined as its root mean square radius. In terms of the momentum-space wave function of the pair, $\chi(\vec{k})$, we have

$$\xi^2 = \int d^3k \frac{\partial \chi^\dagger(\vec{k})}{\partial \vec{k}} \frac{\partial \chi(\vec{k})}{\partial \vec{k}} \bigg/ \int d^3k \chi^\dagger(\vec{k}) \chi(\vec{k}) . \quad (25)$$

In the Bethe-Salpeter equation, the pair wave function can be expressed in terms of the residue of the two-particle propagator at its pole. By analogy, we argue that here we can obtain the (un-normalized) pair wave function as the residue of the anomalous propagator $F(k)$ at its pole,

$$\chi(\vec{k}) = \frac{1}{2\pi i} \int d\omega F(\vec{k}, \omega) e^{i\omega 0^+} , \quad (26)$$

where we retain only the contribution of the positive-energy pole, to be consistent with the vacuum truncation discussed earlier. In Fig. 7, we plot the inverse of the coherence length, $1/\xi$, at $k_F=0.5 \text{ fm}^{-1}$, as a function of the position of virtual or bound state in the vacuum, just as was done in Figs. 5 and 6. Here too, we observe a similar strong correlation. What is most important at the moment, however, are the typical values obtained for the coherence length. We observe that, in the range of calculations shown, these never fall below 3 fm. Near the physical position of the virtual state, the value of the coherence length lies between about 4 to 10 fm. As will be seen shortly, the Fermi momentum at which we have shown the various correlations is close to that for which the coherence length of the pair attains its minimum value. Thus we can claim that the coherence length of the physical bound pair never becomes smaller than about 4 fm.

We can thus justify the correlations observed with the following argument: For the parameter sets of physical interest, the size of a bound pair at low density is much greater than the range of the interaction. As the short-range pair correlations are about the same for all sets of finite-range interaction parameters, it is then a single parameter, the net attraction, that determines the differences in the binding energy of the pair obtained with each of the parameter sets. It suffices to fix the size (or energy) of the pair at one value of the density to obtain its trend over the entire range of values for which the details of the interaction can be neglected. We choose to fix the net attraction between pairs by fixing the position in the complex momentum plane of the 1S_0 virtual state in the vacuum. As we have seen, this is equivalent to fixing the two-nucleon singlet scattering length.

We thus fix a momentum cutoff for each parameter set so that it places the 1S_0 virtual state at its physical location of $k_v \approx -0.05i \text{ fm}^{-1}$. This is impossible for the σ - ω interaction parameters of Ref. [18], for which $ik_v \gtrsim 0.08 \text{ fm}^{-1}$ for $\Lambda \gtrsim 500 \text{ MeV}/c$. In this case, we fix the virtual state at $k_v \approx -0.08i \text{ fm}^{-1}$, its closest point to the physical location. The pairing fields that result are then fairly consistent among themselves and with the non-relativistic result of Ref. [30] for low values of the Fermi momentum, as can be seen in Fig. 8. Our results are also very similar to those obtained in many other non-relativistic calculations of both nuclear matter and neutron matter (for which the gap function is from 10% to 20% larger), which are not shown here [9,15,16]. Although the calculations shown are restricted to those using the σ - ω parameter sets, the gap functions obtained using the σ - ω - π - ρ interaction parameters are quite similar. Even the zero-range model can describe the behavior of the Fermi-momentum gap-function at low densities, when it used with an appropriate cutoff Λ .

We note that the good agreement between different sets of interaction parameters does not extend up to densities at which the magnitude of the pairing fields begins to decrease. There, differences in the details of the interplay between attraction and short-range repulsion become important, introducing a more elaborate dependence on the parameter sets. To the extent to which these details are reflected in the short-range correlations, that is to say, in the momentum dependence of the pairing fields, we can compare this momentum dependence with that of the half-on shell singlet T-matrix to choose the most ‘‘physical’’ parameter sets. As we have not performed relativistic calculations of the T-matrix, we have compared the non-relativistic calculations using the Bonn potential to our gap functions to conclude that the σ - ω and σ - ω - π - ρ parameter sets of Ref. [19] are equally good and are the most ‘‘physical’’ of those we have studied. The half-on-shell singlet T-matrix obtained using the Bonn potential and the gap function obtained using the σ - ω parameters of Ref. [19] are shown in Figs. 3 and 4.

We show in Fig. 9 the coherence lengths ξ obtained using the physical values of the momentum cutoff that resulted in the gap functions of Fig. 8. We observe that the coherence length drops rapidly from infinity, at low densities, to reach a minimum of about 5 fm at about 1/10 the density of saturated nuclear matter. It rises again rapidly, becoming infinite at the density at which pairing disappears. The minimum coherence length is fairly independent of the interaction parameters and is about 5 or 6 fm in all cases studied. The coherence length in neutron matter displays a very similar dependence on the Fermi momentum k_F but is about 10% smaller than in nuclear matter of the same Fermi momentum.

We conclude by interpreting the spatial form of a bound 1S_0 pair in nuclear matter, when it exists, in terms of the magnitude and form of the pairing field, $\Delta(k)$. The short-range correlations of the pair, characterized by the form

of the pairing field, $\Delta(k)/\Delta(0)$, are almost independent of model parameters, momentum cutoff and nuclear density, and are almost identical to those of the two-nucleon 1S_0 virtual state in the vacuum. The asymptotic nature of the pair, is roughly determined by the magnitude of the pairing fields at the Fermi momentum, which are strongly varying functions of the nuclear matter density. Based on the variations observed in the pair coherence length, we estimate that a 1S_0 pair in nuclear matter is most tightly bound at about 1/10 the nuclear saturation density, somewhat below the density for which the pairing fields reach their maximum values. For larger and smaller values of the density, the pair is larger in extent and less bound.

FINAL REMARKS

Our numerical results indicate that the two principal physical ingredients that fix the form and magnitude of the pairing fields and the gap function are the energy of the nucleon-nucleon virtual state and the momentum dependence of its vertex function or, equivalently, the two-nucleon singlet scattering length and the momentum dependence of the half-on-shell zero-energy singlet T-matrix. The short-range two-nucleon correlations contained in the momentum dependence of the pairing fields and the virtual state are determined by the interplay between the short-range repulsion and medium-range attraction of the nucleon-nucleon interaction. If the short-range correlations are held fixed, the magnitude of the pairing fields and the position of the virtual state depend only on the overall strength of the interaction.

Pairing is also expected to occur in the 3S_1 - 3D_1 deuteron channel. This possibility has been investigated by two groups [11,13,30], which both obtained nonrelativistic S-D gap functions that reach values of about 10 MeV. Although we have not performed such calculations, we note that the large values obtained for the S-D gap function are not surprising, given the correlation we observed in Fig. 5. Since the deuteron is a bound pair while the 1S_0 two-nucleon state is virtual, the stronger effective two-nucleon potential in the 3S_1 - 3D_1 channel would also be expected to produce a much larger gap function and pairing fields.

Several recent works have pointed out that medium polarization effects result in an important renormalization of the effective (non-relativistic) nucleon-nucleon interaction [34–36]. One of the observed effects of this renormalization is a large reduction in the magnitude of the gap function. Such a reduction is consistent with our results if the polarization effects of the medium reduce the attraction of the effective two-nucleon potential. Another recent study has shown that the quark substructure of the nucleons and exchanged mesons is also expected to lead to a less attractive two-nucleon potential [37]. We plan to extend our study of pairing to next take into account such effects.

ACKNOWLEDGEMENTS

B.V. Carlson and T. Frederico acknowledge the support of the Conselho Nacional de Desenvolvimento Científico e Tecnológico - CNPq, Brazil.

-
- [1] A. Bohr, B.R. Mottelson and D. Pines, Phys. Rev. **110**, 936 (1958).
 - [2] V.J. Emery, Nucl. Phys. **12** (1959) 69.
 - [3] V.J. Emery, Nucl. Phys. **19** (1960) 154.
 - [4] V.J. Emery and A.M. Sessler, Phys. Rev. **119**, 248 (1960).
 - [5] P.U. Sauer, A. Faessler, H.H. Wolter and M.M. Stingl, Nucl. Phys. **A125**, 257 (1969).
 - [6] A. Faessler, P.U. Sauer and H.H. Wolter, Nucl. Phys. **A129**, 21 (1969).
 - [7] S.B. Khadkikar and M.R. Gunye, Nucl. Phys. **A144**, 289 (1970).
 - [8] H. Kucharek, P. Ring, P. Schuck, R. Bengtsson and M. Girod, Phys. Lett. **216B**, 249 (1989).
 - [9] M. Baldo, J. Cugnon, A. Lejeune and U. Lombardo, Nucl. Phys. **A515**, 409 (1990).
 - [10] M. Baldo, J. Cugnon, A. Lejeune and U. Lombardo, Nucl. Phys. **A536**, 349 (1992).
 - [11] M. Baldo, I. Bombaci and U. Lombardo, Phys. Lett. **283B**, 8 (1992).
 - [12] J.M.C. Chen, J.W. Clark, R.D. Davé and V.V. Khodel, Nucl. Phys. **A555**, 59 (1993).
 - [13] M. Baldo, U. Lombardo, I. Bombaci, and P. Schuck, Phys. Rep. **242C**, 159 (1994).
 - [14] M. Baldo, U. Lombardo, and P. Schuck, Phys. Rev. C **52**, 975 (1995).
 - [15] V. A. Khodel, V. V. Khodel and J. W. Clark, Nucl. Phys. **A598**, 390 (1996).

- [16] Ø .Elgarøy , L. Engvik, M. Hjorth-Jensen and E. Osnes, Nucl. Phys. **A604**, 466 (1996).
[17] B.D. Serot and J.D. Walecka, Adv. Nucl. Phys. **16**, 1 (1986).
[18] C.J. Horowitz and B.D. Serot, Nucl. Phys. **A399**, 529 (1983).
[19] A. Bouyssy, J.F. Mathiot, N. Van Giai and S. Marcos, Phys. Rev. C **36**, 381 (1987).
[20] C.E. Price and G.E. Walker, Phys. Rev. C **36**, 355 (1987).
[21] C.J. Horowitz and B.D. Serot, Nucl. Phys. **A464** 613 (1987).
[22] B. ter Haar and R. Malfliet, Phys. Rep. **149C** 207 (1987).
[23] R. Machleidt, Adv. Nucl. Phys. **19**, 189 (1989).
[24] R. Brockmann and R. Machleidt, Phys. Rev. C **42**, 1965 (1990).
[25] D. Bailin and A. Love, Phys. Rep. **107C**, 325 (1984).
[26] B.V. Carlson and T. Frederico, IEAv Preprint, São José dos Campos, Brazil, 1989.
[27] H. Kucharek and P. Ring, Z. Phys. A **339**, 23 (1991).
[28] F.B.Guimarães, B.V.Carlson, and T.Frederico, Phys. Rev. C **54**, 2385 (1996).
[29] W.H. Dickhoff, Phys. Lett. **210B**, 15 (1988).
[30] B.E. Vonderfecht, C.C. Gearhart, W.H. Dickhoff, A. Polls. e A. Ramos, Phys. Lett. **253B**, 1 (1991).
[31] T. Alm, G. Röpke, A. Sedrakian and F. Weber, Nucl. Phys. **A604**, 491 (1996).
[32] L.P. Gorkov, Sov. Phys. JETP **7**, 505 (1958).
[33] R. Machleidt, in "Computational Nuclear Physics 2"; edited by K. Langanke, J.A. Maruhn and S.E. Koonin (1993 Springer-Verlag New-York, Inc.); pg. 1 .
[34] T.L. Ainsworth, J. Wambach and D. Pines, Phys. Lett. **222B**, 173 (1989).
[35] J. Wambach, T.L. Ainsworth and D. Pines, Nucl. Phys. **A555**, 128 (1993).
[36] H.-J. Schulze, J. Cugnon, A. Lejeune, M. Baldo and U. Lombardo, Phys. Lett. **B375**, 1 (1996).
[37] R. Rapp, R. Machleidt, J.W. Durso, and G.E. Brown, Los Alamos archive preprint nucl-th/9706006.

FIG. 1. Pairing fields and gap functions at the Fermi momentum, obtained with the parameters of Ref. [19] at two values of the cutoff parameter, $\Lambda = 2$ GeV/c (solid lines) and $\Lambda = 1$ GeV/c (dashed lines), for the σ - ω model. The fields Δ_0 , Δ_s , and Δ_g , are in decreasing order.

FIG. 2. Pairing fields and gap functions at the Fermi momentum, obtained with a cutoff parameter of $\Lambda = 2$ GeV/c using the parameters of Ref. [18] (dashed lines) and Ref. [19] (solid lines), for the σ - ω model. The fields Δ_0 , Δ_s , and Δ_g , are in decreasing order.

FIG. 3. Normalized pairing fields and gap functions, as a function of the momentum, for several values of the Fermi momentum, obtained with the σ - ω model parameters of Ref. [19] and a cutoff parameter of $\Lambda = 2$ GeV/c. The ratio $t_{10}(k, 0; 0)/t_{10}(0, 0; 0)$ of the Bonn-B 1S_0 half-on-shell T-matrix at zero energy is also shown (short-dashed line).

FIG. 4. Normalized pairing fields and gap functions, as a function of the momentum, at a Fermi momentum of $k_F = 0.5$ fm $^{-1}$, obtained with the parameters of Ref. [18] at two values of the cutoff parameter, $\Lambda = 2$ GeV/c (solid lines) and $\Lambda = 1$ GeV/c (dashed lines), and the parameters of Ref. [19] with a cutoff of $\Lambda = 1$ GeV/c (dotted line), for the σ - ω model. The ratio $t_{10}(k, 0; 0)/t_{10}(0, 0; 0)$ of the Bonn-B 1S_0 half-on-shell T-matrix at zero energy is also shown (short-dashed line).

FIG. 5. The gap function Δ_g at a Fermi momentum of $k_F = 0.5$ fm $^{-1}$ plotted versus the momentum of the bound or virtual state, $-ik_b$, for each set of interaction parameters and cutoff. Calculations with σ and ω mesons and σ , ω , π and ρ mesons are labelled in the figure. The zero-range calculation is labelled ZR.

FIG. 6. The pairing fields Δ_0 and Δ_S at a Fermi momentum of $k_F = 0.5$ fm $^{-1}$ plotted versus the momentum of the bound or virtual state, $-ik_b$, for each set of interaction parameters and cutoff. Calculations with σ and ω mesons and σ , ω , π and ρ mesons are labelled in the figure. The zero-range calculation is labelled ZR.

FIG. 7. The inverse of the coherence length $1/\xi$ at a Fermi momentum of $k_F = 0.5$ fm $^{-1}$ plotted versus the momentum of the bound or virtual state, $-ik_b$, for each set of interaction parameters and cutoff. Calculations with σ and ω mesons and σ , ω , π and ρ mesons are labelled in the figure. The zero-range calculation is labelled ZR.

FIG. 8. Gap functions Δ_g obtained for several sets of σ - ω interaction parameters that have been constrained so as to yield a virtual state close to the physical one. The non-relativistic calculation of Ref. [30], which uses a Reid soft-core potential, is also shown.

FIG. 9. Coherence lengths ξ obtained for the same sets of σ - ω interaction parameters constrained so as to yield a virtual state close to the physical one as in Fig. 8.

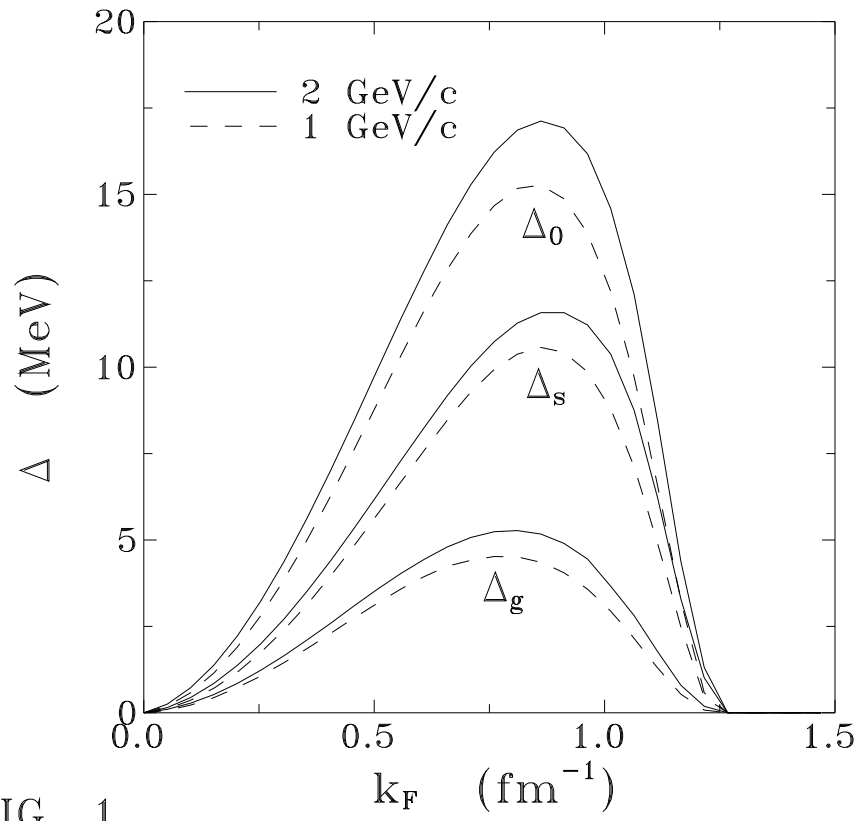


FIG. 1

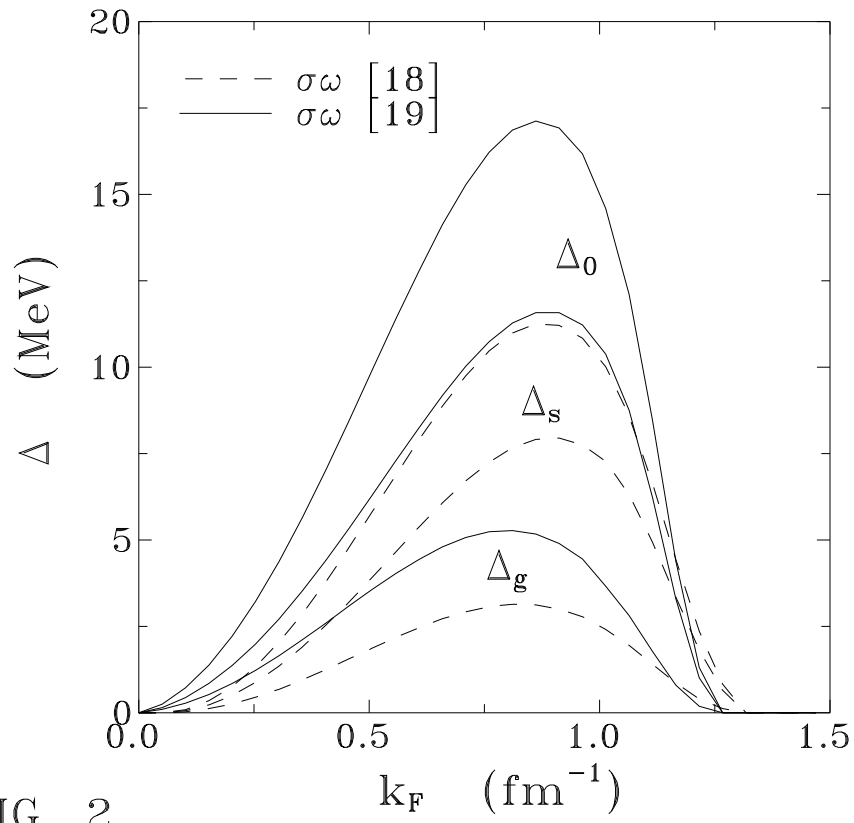


FIG. 2

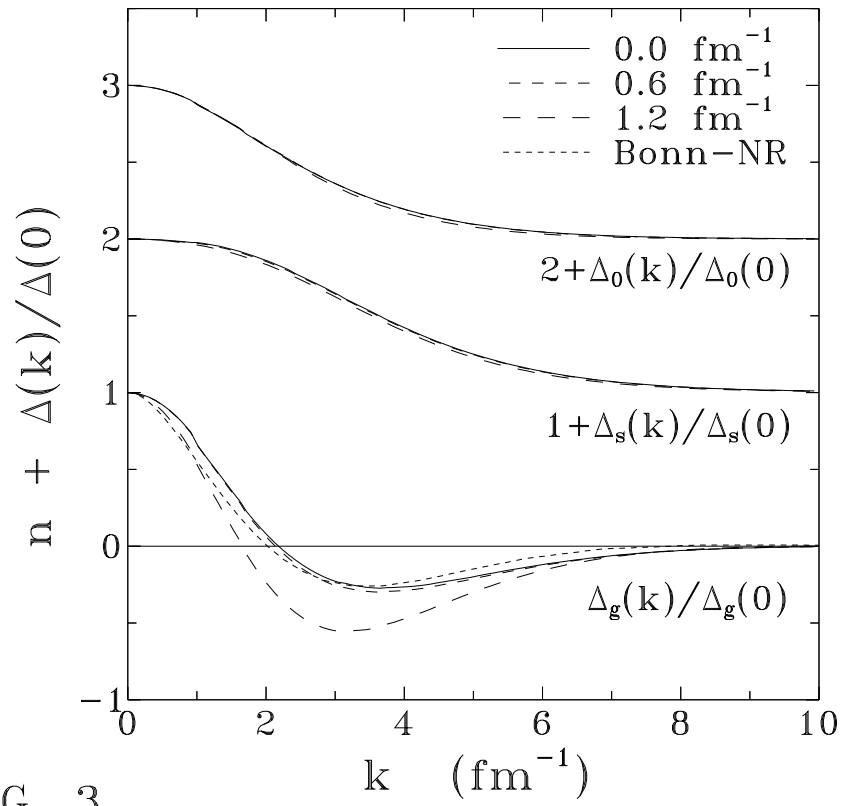


FIG. 3

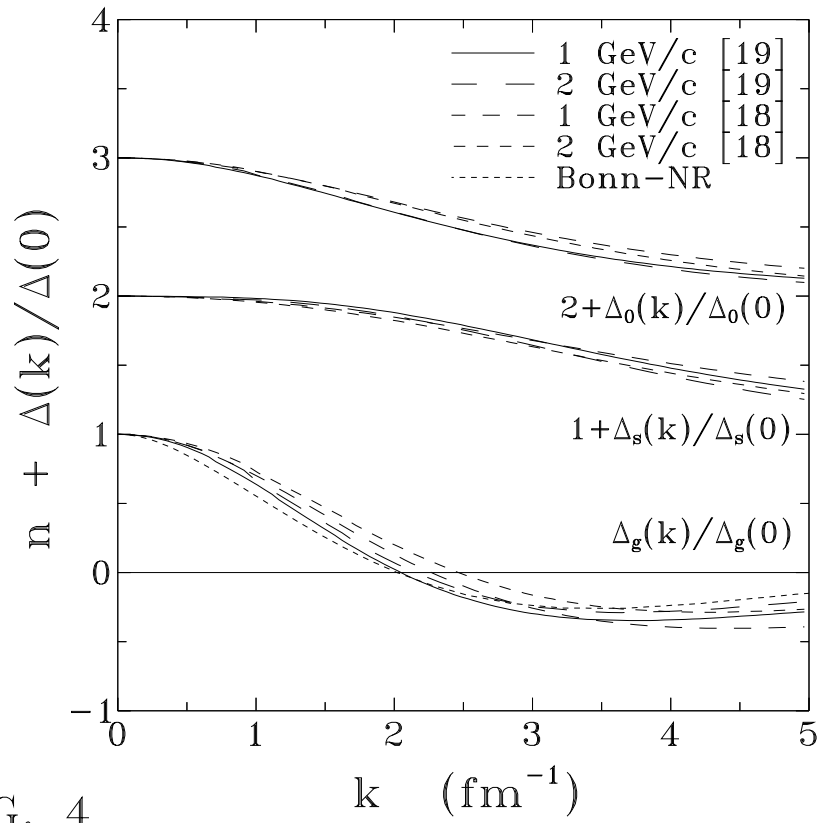


FIG. 4

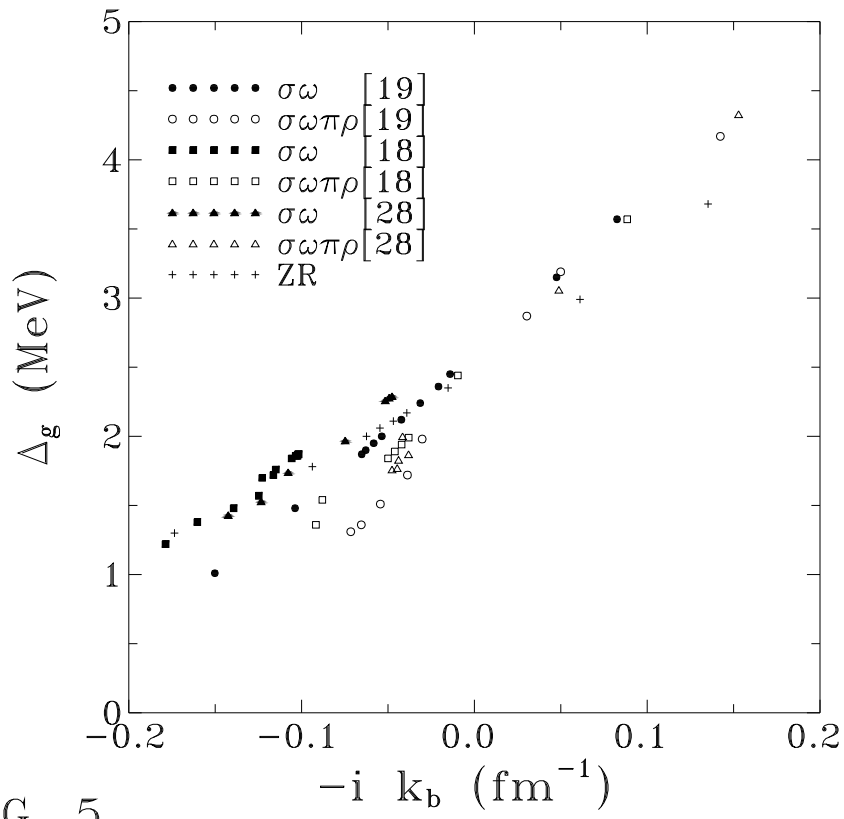


FIG. 5

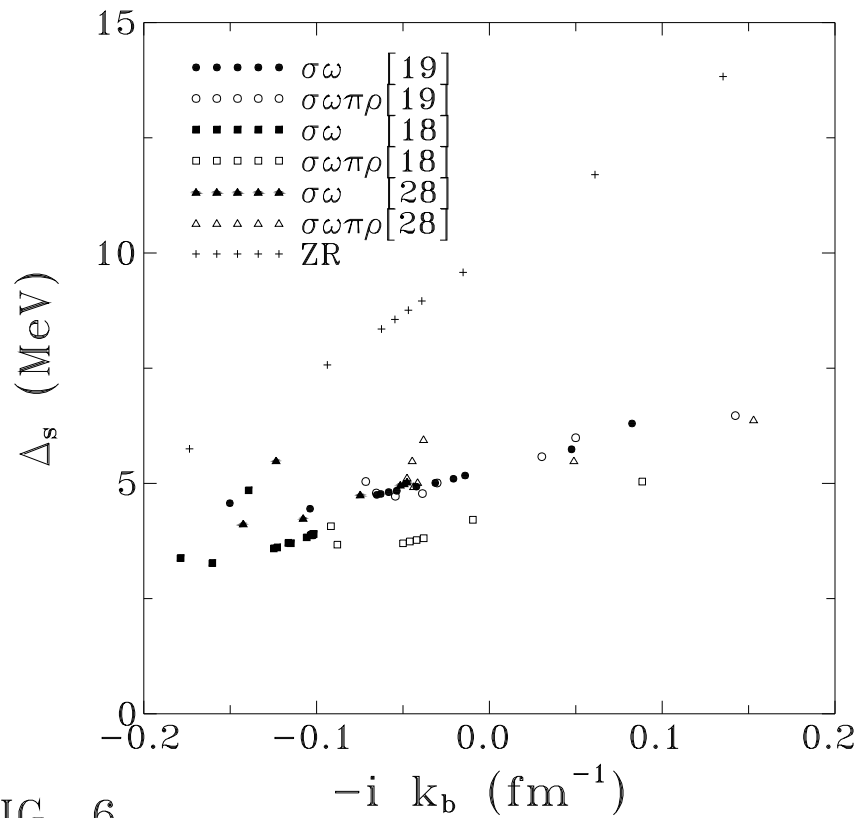
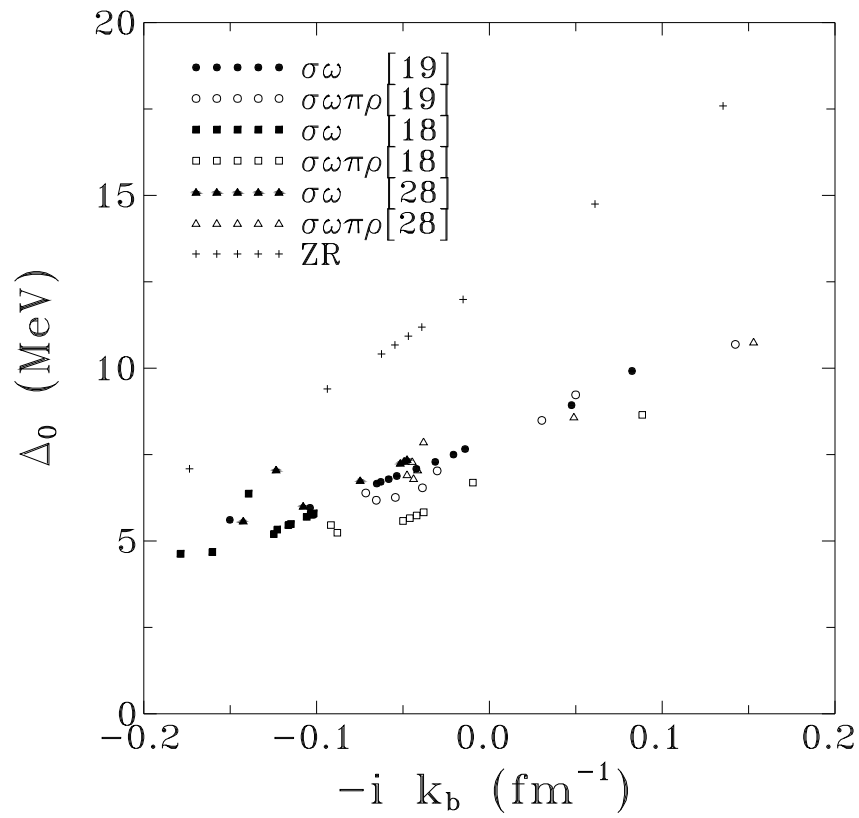


FIG. 6

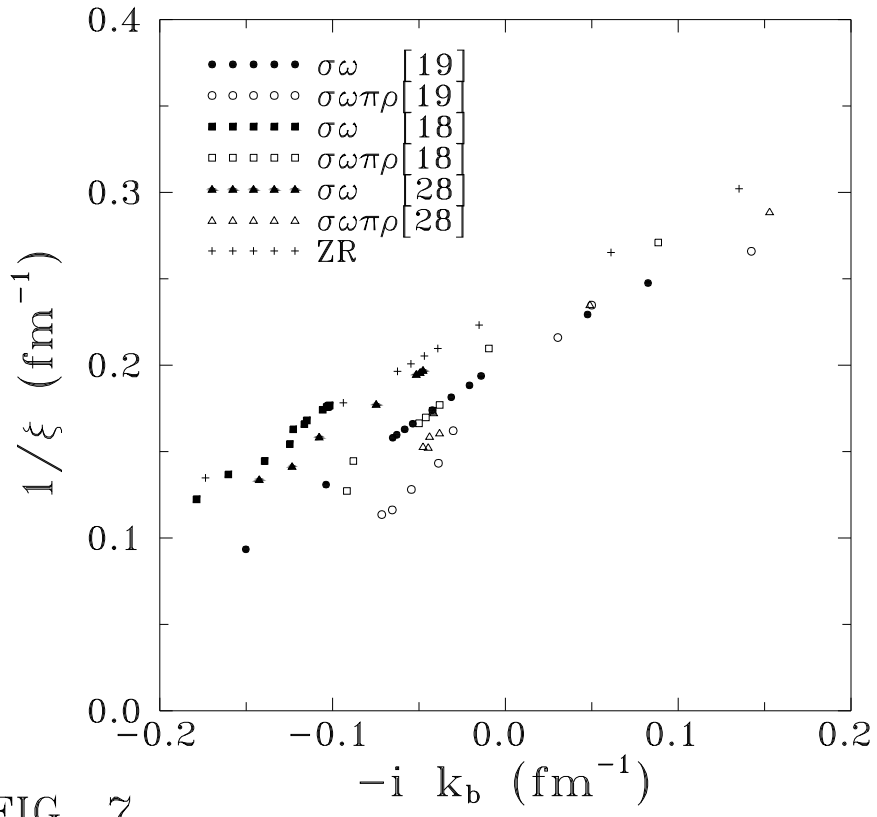
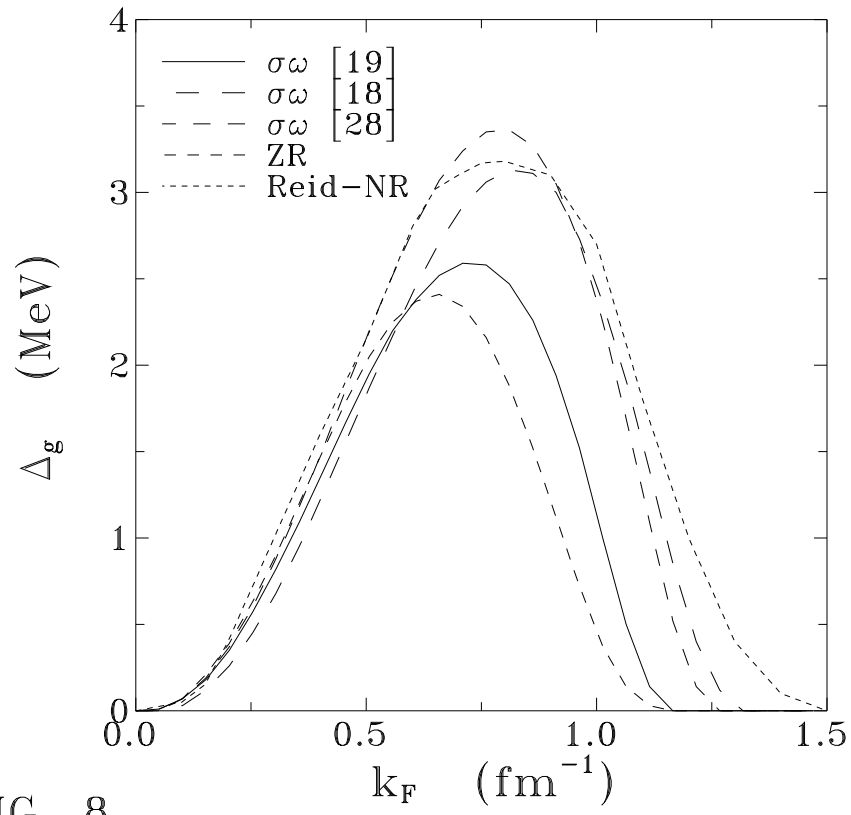


FIG. 7



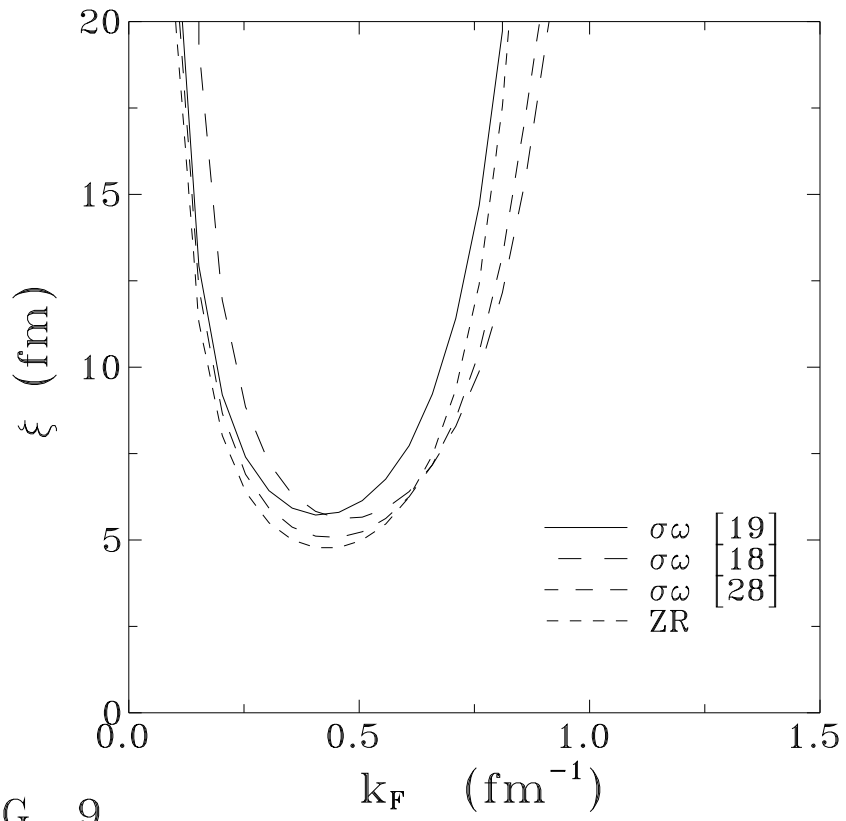


FIG. 9